2022 13th International Symposium on Communication Systems, Networks and Digital Signal Processing (CSNDSP) | 978-1-6654-1044-1/22/$31.00 ©2022 IEEE | DOI: 10.1109/CSNDSP54353.2022.9907971

Towards Illuminating Optical Fiber based Visible Light Communication Uplink

Matej Komanec, Carlos Guerra Yanez, Klara Eollosova, Shivani Rajendra Teli, and Stanislav Zvanovec
Faculty of Electrical Engineering
Czech Technical University in Prague
Prague, Czech Republic 166 27
Email: komanmat@fel.cvut.cz

***Abstract*—We present a novel concept of visible light communication (VLC) uplink by introducing a distributed receiver (Rx) formed by an illuminating optical fiber (IOF) connected to the photodetector. The major functionality of IOF-distributed Rx is to sense/detect the light signal along the fiber span at a range of modulation frequencies coming from an on-off keying modulated light-emitting diode (LED) transmitter. We show that our proposed proof-of-concept of distributed Rx performs below the forward error correction limit of $3.8{\cdot}10^{-3}$ at frequencies up to 400 kHz. We unveil the signal-to-noise ratio (SNR) limit of 19 dB must be maintained for successful data reception. Higher data rates are predicted once the concept is optimized, especially in terms of SNR. The proposed IOF-based scheme can be considered as a solution to the current challenges of VLC uplink.**

I. Introduction

With the current rapid growth of the 5^{th} generation (5G) networks and the rise of Internet of Things (IoT), a broad range of communication technologies is being implemented [1]. Conventional radio-frequency/microwave and fiber-optic systems are being accompanied by visible light communications (VLC) [2], [3] and optical camera communications (OCC) [4]. VLC and OCC bring advantages in terms of immunity to electro-magnetic interference, high channel security and broad unlicensed spectrum. Furthermore, both systems build on low-cost light-emitting diodes (LEDs) as the transmitter (Tx), which simultaneously serve for illumination purposes, thus forming energy efficient communication systems [5]. Additional VLC/OCC functionalities of localization and sensory data transmission can be used in many IoT applications [6], [7].

A VLC/OCC communication channel is typically formed by an LED as a Tx and a photodetector (PD) in the case of VLC or an optical camera in the case of OCC as an Rx. VLC brings significantly higher data rates compared to OCC [8]. Both VLC and OCC are primarily designed for downlink scenarios. The survey in [9] lists the possibilities of providing a VLC uplink using either: i) VLC-VLC links, i.e., using LEDs for both up- and downlink [10]; ii) a WiFi-VLC link such as LiRa with Wifi uplink [11]; and iii) infrared (IR)-VLC link with IR for uplink [12].

Recently, we presented a novel fiber-based OCC system using illuminating optical fibers (IOFs) as a distributed Tx [13], [14]. IOFs are either made of plastic (POFs) [15] or glass material [16] and function on the side-emission effect along the fiber length, where either thanks to material composition or modified waveguiding properties, light leaks out of the fiber (waveguide) in 360° degree thus being an omnidirectional light source. Plastic IOFs are more common with diameters ranging typically from 1-12 mm (nevertheless thinner plastic IOFs can be found). Glass IOFs made of silica with the core diameter below 200 μm were presented first in 2013 [17] and have found a number of applications in fields of medicine [18], biosensing [19] and disinfection [20].

Once we consider VLC systems in combination with fiber optics, optical fiber is most commonly used as a light transport medium from the light source to the point of emission, i.e. light exits (downlink) or enters (uplink) the optical fiber at its end [21].

In this paper, we present a novel concept of IOF-based VLC system working in the uplink scenario. The idea is based on our paper on fiber-based OCC [13], [14] building on the principle of reciprocity; in other words, if an IOF is designed to emit light, it should also capture light. This idea was partially demonstrated in a liquid-level sensing experiment using an IOF [22]. Nevertheless, up to date no one has demonstrated IOF application for upstream data communication links. Such a proposed system might well be employed in various IoT scenarios prohibiting line-of-sight communication where the detection part is distributed in a long span, applications sensitive to radio-frequency interference such as medical facilities, and applications requiring moderate data rates such as a mobile phone user going along e.g. a door frame equipped with IOF or e.g. a car parking in a garage communication with the IOF attached to the walls/pillars.

In this paper, we connect a 1m-long plastic IOF to the PD, which together form a distributed Rx capable of capturing the signal from various directions. An intensity modulated cold-white LED is used as Tx to illuminate the plastic IOF. The link performance is analyzed in terms of bit error rate (BER) and signal-to-noise ratio

(SNR) with respect to varying modulation frequencies (f_s), IOF-to-LED distances (d), and LED rotation/angle (φ). Section II provides the system overview and key devices/parameters, Section III then shows results from light coupling from LED to the IOF, Section IV then presents VLC performance results, and finally Section V brings the conclusion.

II. IOF-VLC System Overview and Measurement Setup

The system overview of the proposed IOF-VLC uplink is illustrated in Fig. 1. An on-off keying (OOK) non-return to zero (NRZ) modulation format is used to modulate the LED. The LED directs its illumination towards the IOF. The LED is equipped with an embedded polymer lens (developed by SQS Fiber Optics) providing a narrow 20° beam pattern. We measured the LED bandwidth to be 1 MHz. As a detector, we use a 1 m-long plastic IOF with 3 mm diameter. On one IOF side, an optical power meter (PM) is attached, later replaced by a PD connected to the oscilloscope (OSC). The LED is facing towards the plastic IOF at a defined distances $d_{\mathrm{A}} = 25$ cm and $d_{\mathrm{B}} = 50$ cm and is placed on a rotation platform with maximum angle $\varphi_{\mathrm{A}} \pm 60°$ and $\varphi_{\mathrm{B}} \pm 40°$, respectively. Maximum LED-IOF distances are for maximum angles as $d_{\mathrm{Amax}} = 50$ cm and $d_{\mathrm{Bmax}} = 65$ cm, respectively. For $\theta = 0°$, the LED faces the IOF exactly at the IOF center (50 cm from PM/PD and 50 cm from the other IOF loose end). Positive angles represent the LED pointing towards the PM/PD side, whereas negative angles stand for the LED pointing towards the IOF loose end. Table I summarizes all key parameters of the used equipment and data modulation.

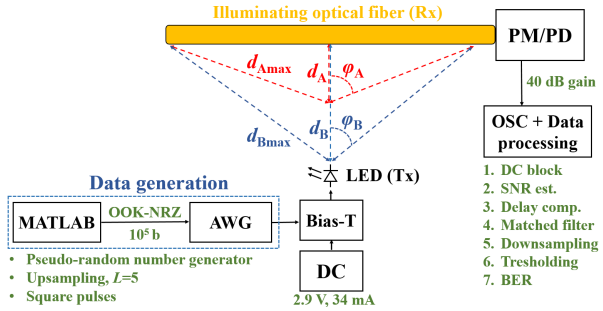

Fig. 1. IOF-VLC system overview.

A photograph of the experimental configuration is shown in Fig. 2. In the experiment, the IOF is in a straight line. The IOF is cut with highest possible precision and is manually aligned with the PD for maximum received optical power, in case of PM we put the IOF into a fast-connector, where optical alignment is automatically ensured. PM/PD with ∼5 cm of the IOF are furthermore covered with a light block to avoid signal entering the PM/PD directly. The LED output beam center is aligned to the IOF and this alignment is preserved during angle tuning.

TABLE I
Key Parameters of the IOF-based VLC System.

Component	Parameter
Receiver	**IOF + PD**
IOF diameter	3.0 mm
IOF material	PMMA
IOF type	ZDEA - Side glow, Super bright
IOF refractive index	1.46 at 589 nm
IOF numerical aperture	0.50
Power meter	Thorlabs PD100 + S150C
Photodetector	Thorlabs PDA100A2
Oscilloscope	Keysight MSOS104A
LED-IOF distance	$d_{\mathrm{A}} = 25$ and $d_{\mathrm{B}} = 50$ cm
Transmitter	**LED**
LED type	Light Avenue - LA CW20WP6
LED surface area	$500 \times 500\ \mu$m
LED bandwidth	1 MHz
LED radiation pattern	20°
Forward current I_F	34 mA
Supply voltage V_s	2.9 V
Data	**On-off keying, non-return to zero**
Modulation frequency f_s	100 - 400 kHz
Modulation voltage (VPP)	0.5 V
Number of bits	10^5
Data generator	Teledyne T3AWG3252
DC power supply	GW Instek, GPD-4303S
Bias-tee	Taylor Microwave, Inc., BT-A11

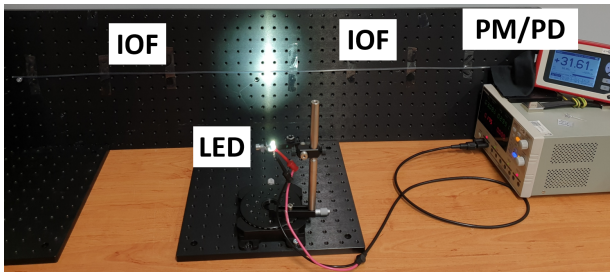

Fig. 2. IOF-VLC link experimental setup with LED facing the IOF center.

III. Analysis of Received Optical Power

In the first step, we analyzed how much optical power can be received from the LED (in a continuous regime without data) in ambient light and complete darkness conditions. We tested two different plastic IOFs of the same diameter and length, denoted as side glow (SG) and super bright (SB). The difference in SG and SB IOF is in their side-emission properties, where SB IOF emits light more intensively, thus should capture more light from the LED.

To reach typical ambient light conditions, the ceiling lighting was set on, generating around -44 dBm at the PM (more specifically -44.6 dBm for side-glow (SG) IOF and -43.4 dBm for super-bright (SB) IOF). In the case of darkness conditions, the detected power level was below -72 dBm. These power levels were then used as a reference before switching the LED on. The LED was operated in the continuous regime at 175 mA and 3 V. Figure 3a depicts the results for the SG IOF, while Fig. 3b shows the results for SB IOF.

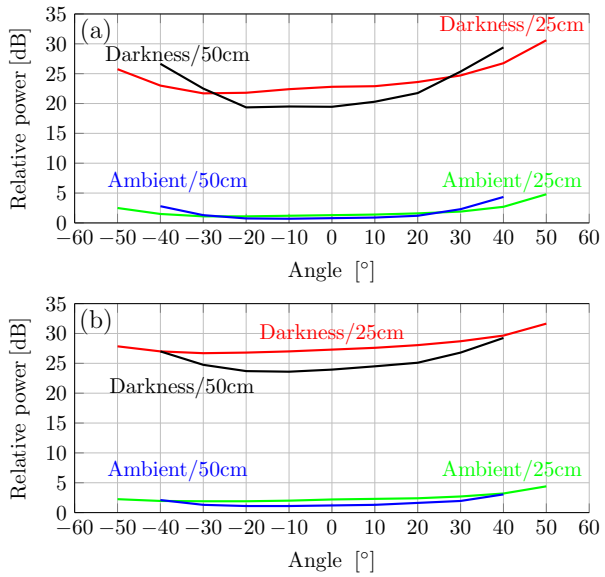

Fig. 3. Measured relative optical power in ambient light and darkness conditions with respect to the LED angle φ for $d_A = 25$ cm and $d_B = 50$ cm , (a) Side-glow IOF, (b) Super-bright IOF.

The biggest difference we can see in the relative optical power under ambient light and darkness conditions, separated by more than 18 dB for both IOFs. In case of ambient light the received optical power is only a few dB above the reference level. This does not mean, that the received optical power from the LED in ambient light is lower than in darkness conditions, only the relative power difference is lower in case of ambient light. To give an example, the LED at 0° angle, 50 cm distance, with a SB IOF provides −19.45 dBm at the PM, which gives 23.95 dB difference to darkness conditions and 1.20 dB difference to ambient light conditions.

What we find interesting is the effect present at the end of the 1 m-long IOF (φ = -50° and -40° for $d_A = 25$ cm and $d_B = 50$ cm, respectively) where the reflection of the IOF/air boundary occurs (approximately 4 %, given the POF refractive index of 1.46) and possibly reflections of other surfaces might couple into the IOF. This effect is more profound in the case of SG IOFs due to their lower fiber attenuation. For SB IOFs, the back reflection is significant only in the case of darkness background and $d_B = 50$ cm.

IV. VLC UPLINK PERFORMANCE

For the VLC upstream evaluation, we selected the SB IOF, as it has a smaller effect of the fiber end-face reflection and an almost constant optical power response to varying LED angle φ.

For the data generation we implemented a MATLAB code producing an OOK NRZ signal with f_s of 100, 200, 300, and 400 kHz. The signal was created using a pseudo-random number generator with a bit sequence of 10^5 bits, upsampled (interpolation factor L=5) and pulse shaped (square pulses). The arbitrary waveform generator (AWG) was then fed with the final signal and via a bias-tee the electrical signal was introduced to the LED. The DC component was set at 2.9 V and 35 mA. The PD was set with a 40 dB gain. The data was captured by the OSC. The signal post-processing used the following procedure: i) DC blocking, i.e. subtracting the signal mean value, ii) SNR estimation, iii) delay compensation to synchronize the data for BER evaluation, iv) matched filtering and downsampling (decimation factor D=5) and finally v) binarization with the threshold at 0 to recover the bits from which the BER was calculated.

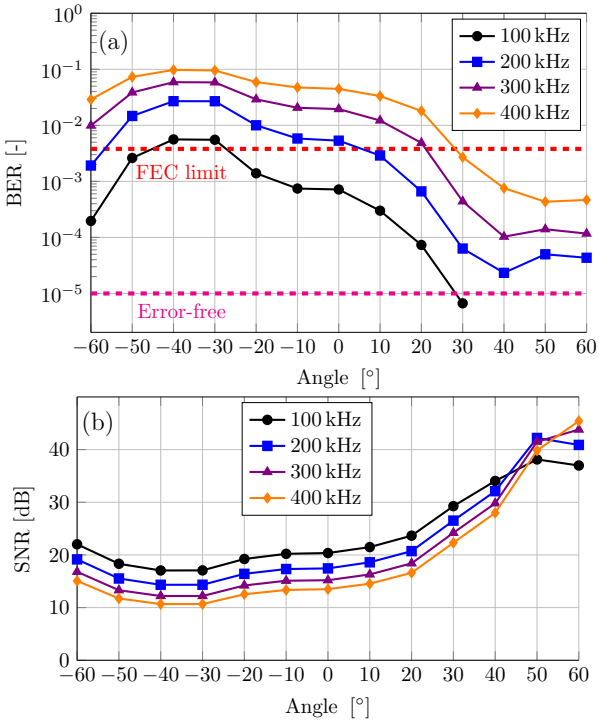

Fig. 4. IOF-based VLC link performance using a 1m-long SB POF with an LED positioned 25 cm away from the IOF center, (a) BER dependence on LED angle, (b) SNR dependence on LED angle.

Figure 4 illustrates the BER and SNR results for the LED located at 25 cm from the IOF, whereas Fig. 5 shows the BER and SNR results for the LED 50 cm away from the IOF. The figures depicting BER values include two limits, first the FEC limit at $3.8 \cdot 10^{-3}$, and second, an error-free limit, which we set based on our data processing limit at $1 \cdot 10^{-5}$ given by the number of generated bits. E.g. for 100 kHz in Fig. 4 for $\varphi \geq +40°$ the BER values are below this error-free limit.

We observe a clear trend both in BER and SNR, where for φ = 0 to +60° (+40° for $d_B = 50$ cm,) there is a gradual improvement in received BER, which is related to the increase of captured light signal, i.e. higher SNR. The worst case is then for φ = -20 to -40° (φ = 0 to -30° for $d_B = 50$ cm,) as the light travels opposite direction with

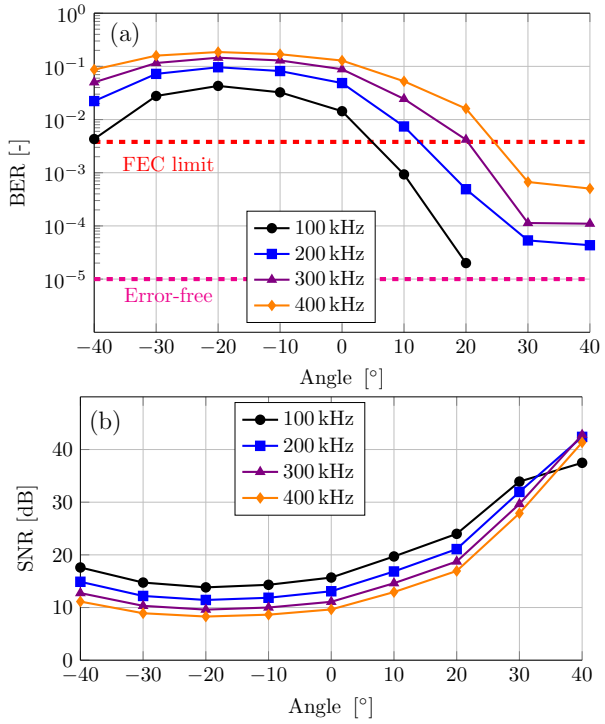

Fig. 5. IOF-based VLC link performance using a 1m-long SB POF with an LED positioned 50 cm away from the IOF center, (a) BER dependence on LED angle, (b) SNR dependence on LED angle

respect to the PD. The SNR threshold limit of 19 dB is required to reach the FEC limit regardless of the signal frequency. Interesting is the BER enhancement at the IOF loose end for both $d_A = 25$ cm and $d_B = 50$ cm, where the back-reflection occurs (as observed in Fig. 3). Furthermore, for $d_A = 25$ cm all BER values are better than for $d_B = 50$ cm. Finally, increasing f_s leads to lower BER/SNR.

V. Conclusion

In this paper, we have demonstrated a novel concept using an illuminating optical fiber acting as a distributed receiver in VLC systems. This setup differs from previous work [14], [13] fundamentally in two aspects: (i) the illuminating fiber is used as a capturing element instead of as an emitter and (ii) the Rx device used is a PD instead of an imaging sensor.

Ambient light effects were first studied for continuous LED regime with regard to received optical power for two IOF variants showing the angular dependence and positive effect of IOF end-face back-reflections.

For our VLC uplink proof-of-concept we used the super-bright plastic IOF with 3 mm diameter and a narrow-beam LED modulated with OOK NRZ signal. We achieved BER below the forward error correction limit for frequencies up to 400 kHz with regard to LED distance from the IOF and LED angle. We revealed that SNR above 19 dB is required to preserve acceptable BER given the FEC limit.

Further system enhancement leads to SNR improvement, which can be achieved by optimizing the IOF-PD coupling and by other IOF-VLC system performance optimizations which are in our future scope and will be presented by the time of the conference.

Acknowledgment

This work was supported by TACR project FW01010571.

References

[1] P. Goyal, A. K. Sahoo, and T. K. Sharma, "Internet of things: Architecture and enabling technologies," *Materials Today: Proceedings*, vol. 34, pp. 719–735, 2021.

[2] Y. Xiao, P. D. Diamantoulakis, Z. Fang, L. Hao, Z. Ma, and G. K. Karagiannidis, "Cooperative hybrid VLC/RF systems with SLIPT," *IEEE Transactions on Communications*, vol. 69, no. 4, pp. 2532–2545, 2021.

[3] F. Delgado-Rajo, A. Melian-Segura, V. Guerra, R. Perez-Jimenez, and D. Sanchez-Rodriguez, "Hybrid RF/VLC network architecture for the internet of things," *Sensors*, vol. 20, no. 2, p. 478, 2020.

[4] M. K. Hasan, M. Shahjalal, M. Z. Chowdhury, and Y. M. Jang, "Access point selection in hybrid OCC/RF Ehealth architecture for real-time remote patient monitoring," in *2018 International Conference on Information and Communication Technology Convergence (ICTC)*. IEEE, 2018, pp. 716–719.

[5] L. Teixeira, F. Loose, C. H. Barriquello, V. A. Reguera, M. A. Dalla Costa, and J. M. Alonso, "On energy efficiency of visible light communication systems," *IEEE Journal of Emerging and Selected Topics in Power Electronics*, vol. 9, no. 5, pp. 6396–6407, 2021.

[6] M. S. Amjad and F. Dressler, "Using Visible Light for Joint Communications and Vibration Sensing in Industrial IoT Applications," in *ICC 2021-IEEE International Conference on Communications*. IEEE, 2021, pp. 1–6.

[7] I. Gokarn and A. Misra, "Adaptive & simultaneous pervasive visible light communication and sensing," in *2021 IEEE International Conference on Pervasive Computing and Communications Workshops and other Affiliated Events (PerCom Workshops)*. IEEE, 2021, pp. 344–347.

[8] S. A. H. Mohsan and H. Amjad, "A comprehensive survey on hybrid wireless networks: practical considerations, challenges, applications and research directions," *Optical and Quantum Electronics*, vol. 53, no. 9, pp. 1–56, 2021.

[9] S. U. Rehman, S. Ullah, P. H. J. Chong, S. Yongchareon, and D. Komosny, "Visible Light Communication: A System Perspective—Overview and Challenges," *Sensors*, vol. 19, no. 5, 2019.

[10] Y. Wang, N. Chi, Y. Wang, L. Tao, and J. Shi, "Network Architecture of a High-Speed Visible Light Communication Local Area Network," *IEEE Photonics Technology Letters*, vol. 27, no. 2, pp. 197–200, 2015.

[11] S. Naribole, S. Chen, E. Heng, and E. Knightly, "LiRa: A WLAN Architecture for Visible Light Communication with a Wi-Fi Uplink," in *2017 14th Annual IEEE International Conference on Sensing, Communication, and Networking (SECON)*, 2017, pp. 1–9.

[12] D. A. Basnayaka and H. Haas, "Hybrid rf and vlc systems: Improving user data rate performance of vlc systems," in *2015 IEEE 81st Vehicular Technology Conference (VTC Spring)*, 2015, pp. 1–5.

[13] S. R. Teli, K. Eollosova, S. Zvanovec, Z. Ghassemlooy, and M. Komanec, "Optical camera communications link using an LED-coupled illuminating optical fiber," *Opt. Lett.*, vol. 46, no. 11, pp. 2622–2625, Jun 2021.

[14] S. R. Teli, K. Eollosova, S. Zvanovec, Z. Ghassemlooy, and M. Komanec., "Experimental Characterization of Fiber Optic Lighting - Optical Camera Communications," in *2021 IEEE 32nd Annual International Symposium on Personal, Indoor and Mobile Radio Communications (PIMRC)*. IEEE, 2021, pp. 1–5.

[15] D. Křemenáková, J. Militký, B. Meryová, and V. Lédl, "Characterization of side emitting plastic optical fibers light intensity loss," *World Journal of Engineering*, vol. 10, no. 3, pp. 223–228, 2013.

[16] S. L. Logunov, K. W. Bennett, E. J. Fewkes, W. S. Klubben, and M. Paniccia, "Silica Nano-Structured Fiber for Illumination," *Journal of Lightwave Technology*, vol. 37, no. 22, pp. 5667–5673, 2019.

[17] S. Logunov, E. Fewkes, P. Shustack, and F. Wagner, "Light diffusing optical fiber for illumination," in *Renewable Energy and the Environment*. Optica Publishing Group, 2013, p. DT3E.4.

[18] W. S. Klubben, S. L. Logunov, E. J. Fewkes, J. Mooney, P. M. Then, P. G. Wigley, H. Schreiber, K. Matias, C. J. Wilson, and M. Ocampo, "Novel light diffusing fiber for use in medical applications," in *Optical Fibers and Sensors for Medical Diagnostics and Treatment Applications XVI*, I. Gannot, Ed., vol. 9702, International Society for Optics and Photonics. SPIE, 2016, pp. 234 – 239.

[19] "Biosensors exploiting unconventional platforms: The case of plasmonic light-diffusing fibers," *Sensors and Actuators B: Chemical*, vol. 337, p. 129771, 2021.

[20] C. Shehatou, S. L. Logunov, P. M. Dunman, C. G. Haidaris, and W. S. Klubben, "Characterizing the Antimicrobial Properties of 405 nm Light and the Corning® Light-Diffusing Fiber Delivery System," *Lasers in Surgery and Medicine*, vol. 51, no. 10, pp. 887–896, 2019.

[21] J. A. Apolo, B. Ortega, and V. Almenar, "Hybrid POF/VLC Links Based on a Single LED for Indoor Communications," *Photonics*, vol. 8, no. 7, 2021.

[22] P. Imperatore, G. Persichetti, G. Testa, and R. Bernini, "Continuous Liquid Level Sensor Based on Coupled Light Diffusing Fibers," *IEEE Journal of Selected Topics in Quantum Electronics*, vol. 26, no. 4, pp. 1–8, 2020.